

Linear momentum transfer in reactions between 140-MeV ^4He ions and heavy nuclei*

V. E. Viola, Jr., C. T. Roche,[†] W. G. Meyer, and R. G. Clark

Department of Chemistry, University of Maryland, College Park, Maryland 20742

(Received 29 July 1974)

The fission of ^{238}U , ^{209}Bi , and ^{197}Au induced by 140-MeV ^4He ions has been studied in order to investigate the target-projectile reaction mechanism. The fission-fragment angular correlation technique was used to measure the linear momentum transfer in these reactions. It is found that an upper limit of $(49.3 \pm 4.4)\%$ of the fission in ^{238}U results from the complete fusion of target and projectile. The incomplete fusion component of the ^{238}U fission cross section includes a large fraction of high linear momentum transfer events, presumably produced in reactions where preequilibrium decay and/or deep knockout reactions are highly probable. The fission of ^{197}Au and ^{209}Bi is found to proceed almost completely via a complete fusion mechanism at this energy. The complete fusion cross section for ^{238}U reactions with 140-MeV ^4He ions is compared with that predicted from semiclassical collision models derived for heavy ion reactions.

[NUCLEAR REACTIONS, FISSION $^{238}\text{U}(\alpha, f)$, $^{209}\text{Bi}(\alpha, f)$, $^{197}\text{Au}(\alpha, f)$, $E = 140$ MeV; measured σ_f , fragment-fragment angular correlation; deduced linear momentum transfer distribution, l_{crit} .]

I. INTRODUCTION

Nuclear reactions between intermediate-energy projectiles and heavy target nuclei have been widely studied in order to determine the influence of large amounts of excitation energy and angular momentum on nuclear behavior. These investigations have yielded an increased understanding of the statistical level properties of complex nuclei and of macroscopic nuclear behavior, as characterized by fission saddle and scission shapes.¹⁻³ The interpretation of phenomena observed in the exit channels of intermediate-energy reactions is, however, frequently complicated by uncertainties in the understanding of the target-projectile interaction mechanism. Because of the many entrance channels available at intermediate bombarding energies—encompassing compound nucleus formation, preequilibrium decay and transfer reactions—a thorough understanding of the mechanism of a given reaction is essential if one is to make a realistic estimate of the excitation energy and angular momentum distributions which characterize the reaction products.

It is well known that for heavy-ion-induced reactions at energies well above the Coulomb barrier the cross section for compound nucleus formation is considerably smaller than the nuclear reaction cross section.^{2,4} Hence, the average excitation energy and angular momentum which characterize the products are correspondingly reduced from calculated values which assume complete fusion of target and projectile in all interactions. The limi-

tation on the cross section for complete fusion in heavy ion reactions is explained in terms of centrifugal and Coulomb forces that become so large beyond some critical value of angular momentum that nuclear attraction is no longer possible.⁵⁻⁹

In reactions induced by intermediate energy ^4He ions, the probability for complete fusion of target and projectile is not nearly as well understood. Kapoor *et al.* studied reactions between 110-MeV ^4He ions and ^{238}U and reported that 91% of the fission cross section could be attributed to complete fusion reactions.¹⁰ In another study of the same system¹¹ using 63.5-MeV ^4He ions, 93% of the reaction cross section was found to proceed by a complete fusion mechanism. These two results suggest that the probability for complete fusion in ^4He -ion-induced reactions is quite high and insensitive to increased bombarding energy; hence, the perturbation of the compound nucleus excitation energy and angular momentum distributions caused by incomplete fusion processes should be small in such reactions. However, other studies^{12,13} have demonstrated a high probability for preequilibrium decay in similar reactions, a conclusion inconsistent with the above interpretation.

The purpose of the present research is to investigate the mechanism of reactions between 140-MeV ^4He ions and heavy target nuclei in order to resolve some of the ambiguities in the interpretation of intermediate energy ^4He -ion reactions. The fission fragment angular correlation technique (Fig. 1) has been used to measure the angle between coincident binary fission fragments. This

angle is related to the linear momentum imparted to the fissioning nucleus by the incident ${}^4\text{He}$ ion. From the angular correlation studies on ${}^{238}\text{U}$ —where nearly all of the reaction cross section results in fission, regardless of the mechanism—a linear momentum transfer distribution is obtained for the reaction products. The resultant linear momentum distribution is interpreted in terms of various complete fusion, preequilibrium decay, and direct reaction mechanisms. In view of these results, the lower-energy results are reexamined. The complete fusion cross section is also compared with that predicted by the critical angular momentum models of Wilczyński⁵ and Bass⁶ in order to test the applicability of macroscopic collision models to ${}^4\text{He}$ -ion-induced reactions.

II. EXPERIMENTAL PROCEDURES

The measurements reported here were performed in a 75-cm diam scattering chamber using a magnetically analyzed and focused beam of 140- and 150-MeV ${}^4\text{He}$ ions from the University of Maryland cyclotron. Isotopically enriched ${}^{238}\text{U}$ and monoisotopic ${}^{209}\text{Bi}$ and ${}^{197}\text{Au}$ targets were prepared

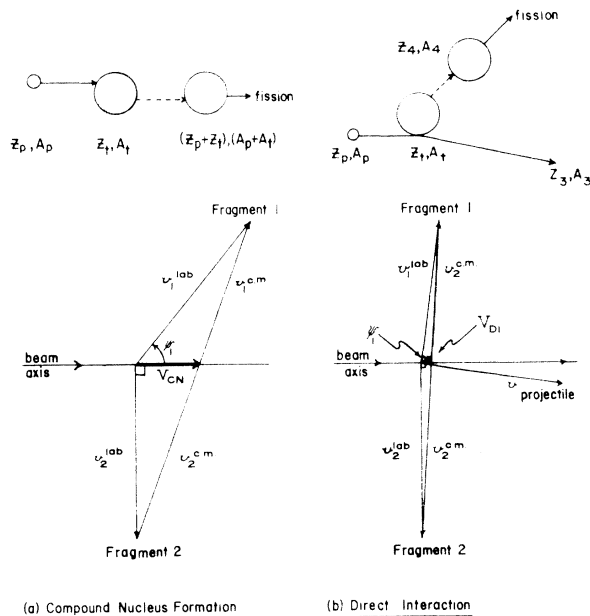


FIG. 1. Schematic and vector diagrams representing binary fission reactions preceded by (a) complete fusion of target and projectile and (b) incomplete fusion. In the vector diagram V is the velocity of the fissioning nucleus and v^{lab} and $v^{\text{c.m.}}$ are the laboratory and c.m. velocities of the fission fragments, respectively. The laboratory angle Ψ_2 for fragment 2 is fixed in these experiments at 270° and Ψ_1 represents the correlation angle of the complementary fragment 1. The c.m. transformation parameter is $x^2 = (V/v^{\text{c.m.}})^2$.

by vacuum evaporation onto carbon films. Target material thicknesses were in most cases 80–140 $\mu\text{g}/\text{cm}^2$ and backing thicknesses ranged from 20 to 100 $\mu\text{g}/\text{cm}^2$. Angular correlations between binary fission fragments were performed using a heavy-ion surface-barrier semiconductor detector placed on one side of the beam axis and a 50×6 -mm position-sensitive semiconductor detector placed at the appropriate correlation angles on the opposite side of the beam axis. The heavy-ion detector served as an angle defining detector for the angular correlation; it was placed 25 cm from the target and at 270° with respect to the beam axis, giving an angular acceptance of $\pm 0.7^\circ$. The position-sensitive detector (PSD) was mounted 15 cm from the target and intercepted approximately $\pm 10^\circ$ of the reaction plane. It was covered by a 15-slit collimator, each slit having an angular acceptance of $\pm 0.2^\circ$. Appropriate corrections for angular geometry were applied to the data derived from this arrangement and amounted to less than 4.3% in all cases. Both detectors were calibrated with a ${}^{252}\text{Cf}$ spontaneous fission source.

Both planar and nonplanar angular correlations were measured. The planar measurements were performed with the longitudinal axis of the PSD in the reaction plane formed by the beam, target, and defining detector. Both detectors were kept at fixed angles during successive measurements of each of the three targets. This procedure preserved the systematic accuracy of the angular correlations with respect to one another, which was an important consideration in analysis of the data (Sec. III). Targets were alternated by means of a remote-controlled target ladder, which maintained the target angle at 45° to the beam. For ${}^{197}\text{Au}$ and ${}^{209}\text{Bi}$ targets the entire planar angular correlation function could be measured for one setting of the PSD angle; for ${}^{238}\text{U}$ three overlapping angular settings were necessary. These measurements were performed for two separate sets of ${}^{197}\text{Au}$, ${}^{209}\text{Bi}$, and ${}^{238}\text{U}$ targets in order to test for possible effects of target thickness, accidental rates, and angular inconsistencies on the data. The results of the two sets of measurements agreed to within $\pm 0.1^\circ$ for the most probable correlation angle and $\pm 0.2^\circ$ for the full width at half-maximum (FWHM) of the correlation function.

Nonplanar measurements were performed by rotating the PSD to a position perpendicular to the reaction plane. The nonplanar measurements were necessary to insure that reactions which did not involve formation of a compound nucleus and which possessed linear momentum components out of the reaction plane were properly taken into account. For the ${}^{238}\text{U}$ target, which exhibited a high probability for incomplete linear momentum transfer

events in the planar measurements, nonplanar correlations were measured at 2° intervals from 68° to 92° . Most of these measurements were performed with 150-MeV ^4He ions, but comparison of results with 140-MeV bombardments showed them to be the same within the limits of experimental error. Because the ^{197}Au and ^{209}Bi targets showed little evidence for noncompound nucleus events, nonplanar measurements were made only at the most probable correlation angle.

The three coincident signals from each event—PSD energy and position and defining detector energy—were amplified using standard charge-sensitive preamplifiers and shaping amplifiers and then fed into 1024-channel analog-to-digital converters. Coincidence gating was performed using a time-to-amplitude converter. The data were stored sequentially on magnetic tape and processed on-line using the IBM 360/44 computer at the Maryland Cyclotron Laboratory. The results presented here are restricted to the position-energy portion of the data. The energy-energy correlations will be analyzed in a subsequent publication.

In order to obtain the absolute value of the complete fusion cross section, the total fission cross section for ^{238}U bombarded by 140-MeV ^4He ions was also measured in these experiments. Fission fragments from three ^{238}U targets of thicknesses 162, 165, and $498 \mu\text{g}/\text{cm}^2$, respectively, were counted with two separate heavy-ion semiconductor detectors, each with an accurately determined geometry. Spectra were recorded at two different angles for each detector and target. From a knowledge of the integrated beam current, counting rates, geometries, target thicknesses, and fragment angular distributions (measured in a separate set of experiments), a total fission cross section of

$$\sigma_f = 2760 \pm 244 \text{ mb}$$

was determined.

III. DATA ANALYSIS

The comparative results of the fission-fragment angular correlation measurements for the three systems studied in this work are shown in Fig. 2, which presents the planar angular correlation data, and Fig. 3, which is a contour diagram showing both the planar and nonplanar components of the angular correlations. The correlation parameters derived from the data are summarized in Table I. The calculated most probable correlation angle, Ψ_{mp} , for reactions in which a compound nucleus is formed are indicated by arrows in Fig. 2 and dots in Fig. 3 for each target. The relative error in the correlation angles for the three targets is $\pm 0.1^\circ$ and the absolute angles are known to $\pm 0.3^\circ$. For reactions induced in heavy elements by 140-MeV ^4He

ions, the intrinsic linear momentum of the fissioning nucleus p_{fN} can be expressed in terms of the correlation angle Ψ (as defined in Fig. 1) by the approximate function

$$p_{\text{fN}} \propto (\frac{1}{2}\pi - \Psi_1),$$

where $\Psi_1 = \Psi_{\text{mp}}$ represents complete momentum transfer and $\Psi_1 = \frac{1}{2}\pi$ represents zero momentum transfer, assuming the defining detector angle Ψ_2 is $-\frac{1}{2}\pi$. An inherent dispersion in the correlation functions for a given value of p_{fN} arises from the kinematic effects of two factors: (1) mass asymmetry of the fragments, which favors a slight skewing in the direction of low values of Ψ , and (2) neutron evaporation from the fissioning nucleus or fragments, which is symmetric in nature. At

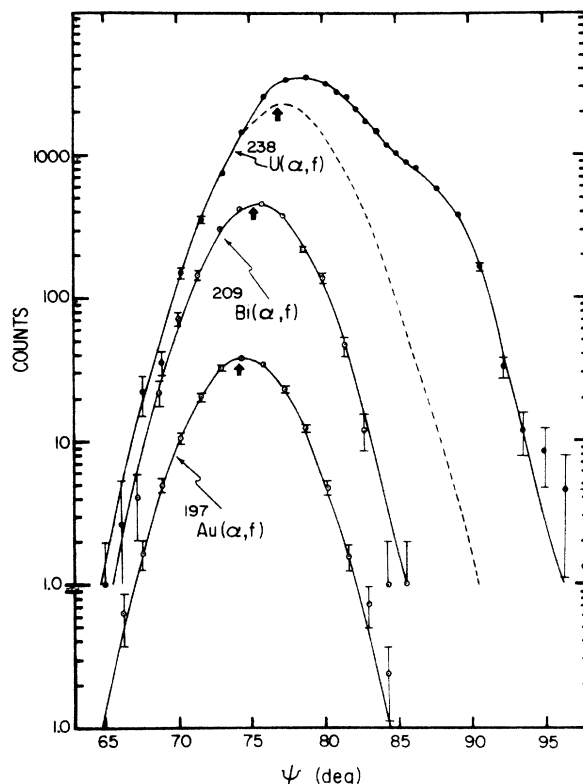


FIG. 2. Angular correlations for the fission of ^{238}U , ^{209}Bi , and ^{197}Au with 140-MeV ^4He ions. Data were taken in the reaction plane and represent the coincidence counting rate as a function of correlation angle Ψ defined in Fig. 1. Arrows indicate the position of the most probable correlation angle calculated from kinematics for each system. The solid curves for the ^{209}Bi and ^{197}Au targets (data: open circles) are empirically fitted functions described in the text. The dashed curve for ^{238}U fission is that predicted from systematics for fission following complete fusion. The solid curve for ^{238}U is calculated from the linear momentum distribution shown in Figs. 6 and 7.

the bombarding energy and linear momentum considered in this work, the effect of neutron evaporation is expected to be dominant, thus leading to the prediction of nearly symmetric correlation functions for events which proceed via a complete fusion mechanism.

From examination of the ^{209}Bi and ^{197}Au data it is concluded that the fission induced in these nuclides by 140-MeV ^4He ions proceeds primarily via a complete fusion mechanism. The most probable correlation angles for these two systems coincide with the values calculated under the assumption of compound nucleus formation, within the limits of experimental error. Further, the correlation functions are symmetric about the most probable correlation angle, whereas if any appreciable amount of fission resulted following incomplete momentum transfer, these functions would be skewed toward 90° . This conclusion does not agree with the conclusions of Bimbot and LeBeyec¹³ from

studies of intermediate energy reactions in lead isotopes. The ^{197}Au and ^{209}Bi angular correlation functions are described well by an empirical function of the form

$$y = Ae^{-bx^n}.$$

Here y is the correlation coincidence rate and x is the absolute value of the deviation in angle from the most probable value, $x = |\Psi - \Psi_{\text{mp}}|$. The constant A is related to the coincidence rate and b to the FWHM of the distribution. These functions have been normalized to the data using $n = 1.94$ and 1.87 for gold and bismuth, respectively, and are the basis for the solid lines in Fig. 2. The shape of the nonplanar angular correlations (for constant Ψ) for bismuth and gold follow the same functional behavior as the planar data within the limits of error, although there is some indication that the planar correlation is slightly broader, as might be expected from the effects of fragment mass asymmetry.

From comparison of the angular correlation for uranium fission with the gold and bismuth results in Figs. 2 and 3, it is evident that reaction mechanisms other than complete fusion contribute significantly to the total fission cross section for ^{238}U . This fact is demonstrated more directly in the fragment kinetic energy distributions shown in Fig. 4. For a correlation angle of $\Psi = 77.5^\circ$ a broad single peak is observed in the fragment energy spectrum, indicative of high energy fission, whereas for $\Psi = 90.3^\circ$ an asymmetric fragment distribution is observed, characteristic of low-energy fission.

In order to estimate the relative contributions of complete fusion (CF) versus incomplete fusion (ICF) reactions, we have utilized the systematic behavior of the angular correlation functions for fission reactions in which complete fusion can be clearly distinguished. The gold and bismuth data

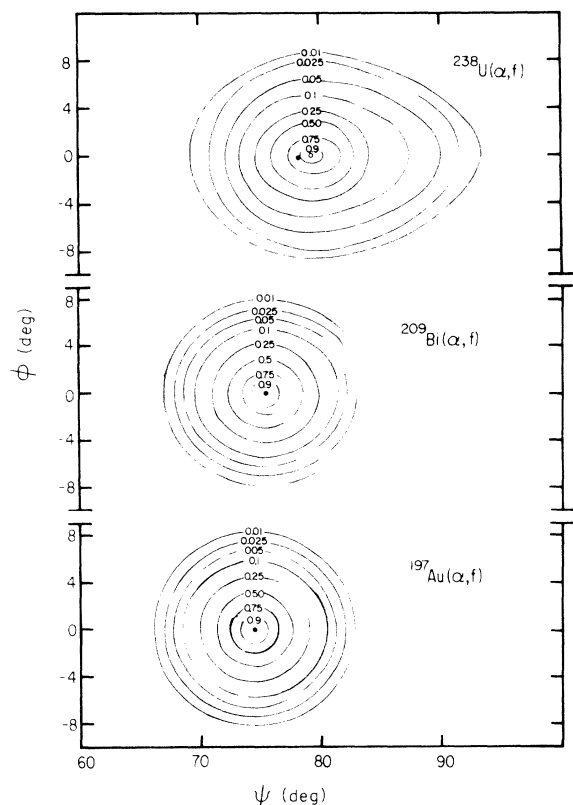


FIG. 3. Contour diagram of angular correlations for ^{238}U , ^{209}Bi , and ^{197}Au systems. The planar angle is represented by Ψ and the nonplanar angle is given by ϕ . Contours are labeled in terms of the fraction of events at a given angle pair with respect to the most probable correlation angle. The most probable correlation angle predicted by kinematics is shown as a closed circle on each diagram.

TABLE I. Summary of fission-fragment angular correlation parameters derived from data shown in Figs. 2 and 3. The relative angular accuracy between the three target systems is $\pm 0.1^\circ$ and the absolute error in the knowledge of the detector angles Ψ is $\pm 0.3^\circ$. Full width at half maximum (FWHM) values for the correlations have an error of $\pm 0.2^\circ$ in each case.

	^{197}Au	^{209}Bi	^{238}U
Most probable correlation angle Ψ_{mp}			
Experimental (deg)	74.5	75.5	78.5
Calculated (deg)	74.2	75.2	76.9
FWHM			
Planar (deg)	6.4	6.2	7.9
Nonplanar (deg)	6.2	6.1	6.9

from the present studies have been used to predict the angular correlation properties for the ^{238}U target, i.e., a most probable correlation angle of $\Psi_{\text{mp}} = 77.2^\circ$ and a FWHM = 6.5° for fission following compound nucleus formation. These parameters are consistent with the results of heavy-ion-induced fission studies⁴ where the reaction kinematics permit clear separation of complete fusion and incomplete fusion events. The heavy-ion correlation functions are characterized as follows: (1) Excellent agreement is found between the kinematically predicted and experimental values of Ψ_{mp} and (2) for a given projectile and bombarding energy, the FWHM of the angular correlation is nearly independent of target nuclide for ^{197}Au , ^{209}Bi , and ^{238}U fission. Using these assumptions, a correlation function

$$y = A \exp(-0.0858x^{1.77})$$

is derived to account for fission following compound nucleus formation in reactions of 140-MeV ^4He ions with ^{238}U . The normalization constant A is determined using the kinematic restriction that the lowest angles Ψ of the correlation function in

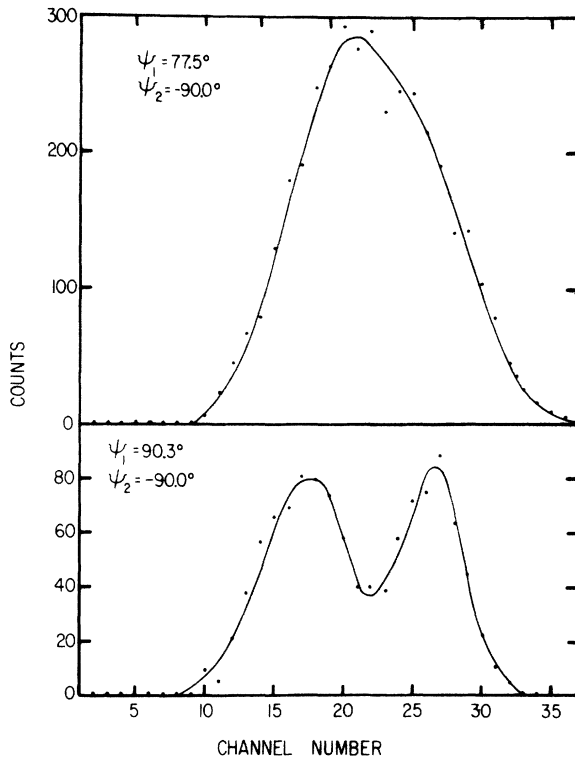


FIG. 4. Kinetic energy distribution for fission fragments produced in bombardment of ^{238}U with 140-MeV ^4He ions. Upper curve with $\Psi_1 = 77.5^\circ$ and $\Psi_2 = 270^\circ$ represents high energy fission. Lower curve, for which $\Psi_1 = 90.3^\circ$ and $\Psi_2 = 270^\circ$, is characteristic of low energy fission.

Fig. 2 must correspond to complete momentum transfer reactions. This function is plotted as the dashed curve in Fig. 2.

IV. RESULTS

A. Complete fusion cross section

By integrating over the entire reaction surface in Fig. 3 for both total experimental events and predicted complete fusion events, the upper limit for the complete fusion cross section in reactions between 140-MeV ^4He ions and ^{238}U is

$$\sigma_{\text{CF}} = (0.493 \pm 0.044) \sigma_{\text{R}} = 1361 \pm 120 \text{ mb}.$$

Here we assume that because of the high fissionability of ^{238}U , the total reaction cross section σ_{R} is equal to the total fission cross section σ_{f} . Error limits are based on an estimated possible error of $\pm 0.1^\circ$ in Ψ_{mp} and $\pm 0.5^\circ$ in the FWHM for the complete fusion correlation function. It should be noted that if the CF correlation function for ^{238}U is broader than for ^{209}Bi and ^{197}Au , which might result due to the greater mass asymmetry and somewhat higher excitation energy for the ^{238}U system, then our value for σ_{CF} will be lower yet.

Our result is in major disagreement with the value of $\sigma_{\text{CF}} = 0.91\sigma_{\text{f}}$ determined by Kapoor, Baba, and Thompson¹⁰ at 110 MeV. However, reexamination of the data in Ref. 10 reveals that the peak of

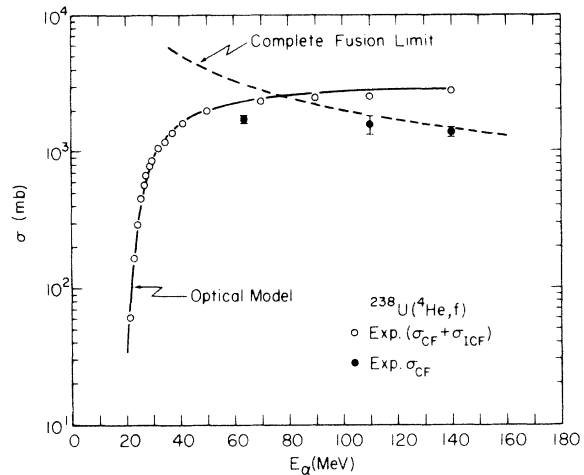


FIG. 5. Total fission and complete fusion cross sections for reactions between α particles and ^{238}U . Open circles are total fission cross sections (assumed equal to nuclear reaction cross section); data are taken from Ref. 14 (up to 42 MeV); from Ref. 10 (50–110 MeV) and the present work (140 MeV). Solid points are complete fusion cross sections discussed in Sec. IVA. Solid curve is optical model fit to the nuclear reaction cross section and dashed curve is complete fusion cross section calculated from the Wilczyński model, as discussed in text.

the ^{238}U fission fragment correlation function is displaced approximately 1.5° , nearer 90° than the calculated value for a complete fusion reaction. On the other hand, the ^{209}Bi fission correlation function obtained in Ref. 10 agrees quite well with the calculated value. The ^{238}U discrepancy was overlooked in the analysis of the 110-MeV data. If the 110-MeV data are treated using the systematics of fission fragment angular correlations as we have done for the 140-MeV data, then a value of $\sigma_{CF}/\sigma_R \cong 0.65 \pm 0.10$ results. The complete fusion cross sections derived from our analysis of angular correlation functions from ^4He -ion induced fission of ^{238}U are plotted in Fig. 5 as a function of bombarding energy. Also shown in Fig. 5 is an optical model fit to the total fission cross sections using the deformed optical model potential of Rasmussen and Sugawara-Tanabe.¹⁵ The parameters for the calculation were the following: well depth, $V_0 = 130$ MeV; radius parameter $r_0 = 1.194$ fm; diffuseness, $d = 0.35$ fm, and deformation parameters¹⁶ for ^{238}U , $\beta_2 = 0.261$ and $\beta_4 = 0.106$. It is observed that the complete fusion cross section decreases with increasing bombarding energy. This fact is discussed further in Sec. IV C.

B. Linear momentum distribution

Comparison of the experimental angular correlation for ^{238}U with that determined assuming complete fusion (Fig. 2) reveals that a considerable fraction of the incomplete fusion events involve large transfers of linear momentum from the projectile to the fissioning nucleus. We interpret this result as evidence of a high probability for pre-equilibrium decay and/or deep knock-out reactions in the nuclear reaction mechanism. This result is consistent with previous workers who have studied spallation product yields in reactions of intermediate energy ^4He ions with heavy elements^{12,13} and with the (α, α') studies of Chenevert, Chant, and Halpern.¹⁷

By further utilizing the angular correlation systematics for ^4He -ion-induced fission reactions, the distribution of linear momenta which characterize the fissioning nuclei in ^{238}U reactions can be derived. For the purposes of this analysis, the linear momentum distribution of the fissioning nuclei was arbitrarily divided into 10 equivalent bins, representing $\frac{1}{10}$ of full momentum transfer, $\frac{2}{10}$ of full momentum transfer, etc. The percentage of complete linear momentum transfer events was taken a priori to be 49.3%, as determined in Sec. IV A. The percentage of events corresponding to the remaining nine linear momentum transfer bins was derived by performing a least squares fit to the incomplete fusion residue of the fission corre-

lation function. In Fig. 6 the calculated correlation functions and their percentage contributions to the experimental results are shown as solid lines. The sum of the 10 calculated correlation functions is given by the dashed line, which is found to reproduce the experimental points well.

In Fig. 7 the percentage of events for each fractional linear momentum transfer bin is plotted. This analysis reinforces the conclusion that high momentum transfer, but incomplete fusion events play an important role in these reactions. In addition, the bump in the histogram corresponding to low momentum transfers presumably reflects the extent to which direct surface reactions contribute to the total cross section.

Independent evidence to support the linear momentum distribution shown in Fig. 7 can be obtained from analysis of the measured fragment angular distributions for 140-MeV ^4He -ion-induced

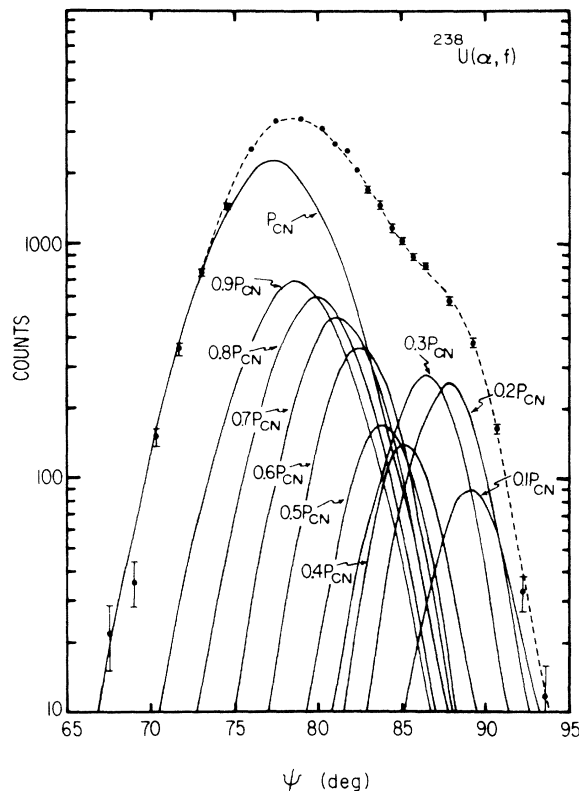


FIG. 6. Linear momentum transfer components which make up fission fragment angular correlation from 140-MeV ^4He -ion-induced fission of ^{238}U . Solid lines refer to angular correlation functions predicted by systematics. Each curve refers to a specific fractional momentum transfer, $0.1p_{CN}$, $0.2p_{CN}$, etc. up to the full momentum transfer, p_{CN} . Points represent the experimental data shown in Fig. 2 and dashed line is the sum of all solid lines.

fission of ^{238}U reported elsewhere.¹⁸ The average center-of-mass transformation parameter x^2 calculated from the momentum distribution in Fig. 7 is $x^2 = 0.743x_{\text{CF}}^2$, where x_{CF}^2 is the transformation parameter appropriate to full momentum transfer events. This is in excellent agreement with the experimental value of $x^2 = 0.74x_{\text{CF}}^2$ required to produce an angular distribution that is symmetric about 90° in the center-of-mass system, which must be the case for binary fission events. A similar analysis of the angular distributions for fission of ^{197}Au and ^{209}Bi in Ref. 18 yielded transformation parameters identical to the value calculated for complete fusion. This is in good agreement with our conclusion that fission induced in the bismuth and gold systems proceeds primarily through a complete fusion mechanism.

Thus, it is apparent from our data that any attempt to derive information about fission from studies using intermediate-energy ^4He ions as projectiles must pay careful attention to the details of

the nuclear reaction mechanism. Otherwise, one cannot possibly understand the distribution of fissioning species, excitation energies, and angular momenta that characterize these reactions.

C. Critical angular momentum

The concept of a centrifugal limitation to the complete fusion of target and projectile has been extensively applied to the analysis of heavy-ion reactions in order to explain the decrease in complete fusion cross sections as a function of bombarding energy for reactions that occur well above the Coulomb barrier.^{5-9,19} This cross section limitation has been parametrized in terms of a critical angular momentum l_c above which the target and projectile cannot coalesce due to centrifugal repulsion. It is not apparent that these semiclassical treatments of nuclear behavior are appropriate to ^4He -ion-induced reactions. However, because of the large binding energy of the α particle, it can be argued that it will maintain its integrity in intermediate-energy reactions, especially for reactions near the nuclear surface. Thus, it may be possible to treat such collisions with macroscopic models. In addition, the excitation function for complete fusion in ^4He -ion induced reactions (Fig. 5) and those observed in heavy-ion-induced reactions¹⁹ are sufficiently similar to warrant comparison with the same type of reaction model.

Several authors⁷⁻⁹ have examined the critical angular momentum appropriate to the exit reaction channel; that is, the angular momentum that corresponds to the disappearance of the fission barrier in the compound system. However, Zebelman and Miller²⁰ have recently performed measurements that indicate complete fusion cross sections are determined by dynamic processes in the entrance reaction channel. Wilczyński⁵ and Bass⁶ have proposed models which apply the concept of dynamic force equilibrium between two touching spherical liquid drops in the entrance reaction channel to determine critical angular momenta and complete fusion cross sections. Both models predict similar behavior for reactions induced by argon and lighter ions and the formalism of Wilczyński is used here.

The attractive nuclear force at contact for two spherical, charged liquid drops is approximated by the surface energy of the two drops. The critical angular momentum is thus determined at the point where the surface tension force is just balanced by Coulomb and centrifugal repulsion. Thus, l_c can be evaluated from the expression

$$2\pi(\gamma_1 + \gamma_2)R_1R_2 = \frac{Z_1Z_2e^2}{(R_1 + R_2)} + \frac{\hbar^2 l_c(l_c + 1)}{\mu(R_1 + R_2)^2}.$$

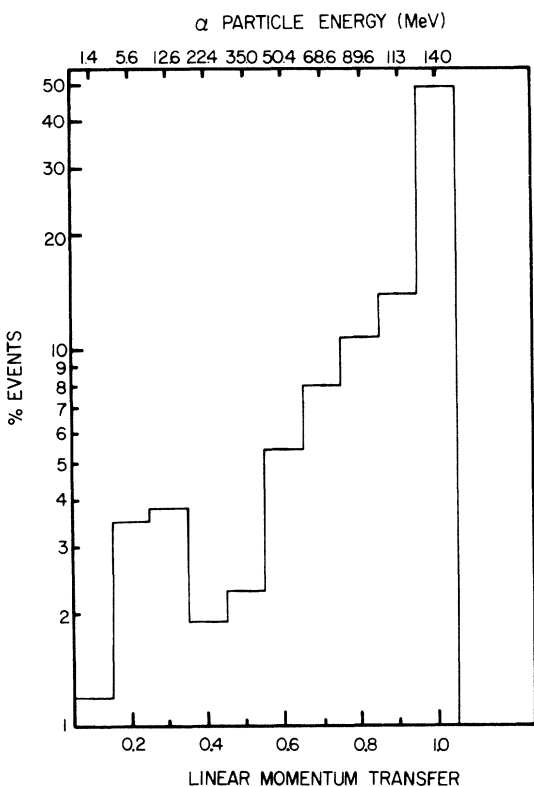


FIG. 7. Linear momentum distribution for fissioning nuclei produced in bombardment of ^{238}U with 140-MeV ^4He ions. The percentage of events is plotted as a function of the ratio of the observed linear momentum transfer to that for complete momentum transfer. Histogram was derived from angular correlation data for ^{238}U and the systematic behavior of angular correlations from other systems, as shown in Fig. 6.

Here γ_i represents the liquid drop surface tension coefficient

$$\gamma_i = \frac{a_s [1 - \kappa(N - Z/A)^2]}{4\pi r_0^2},$$

where a_s and κ are the surface energy and surface asymmetry terms from the semiempirical mass equation. Values of $a_s = 17.9439$ MeV and $\kappa = 1.7826$ were used in these comparisons.⁵ The nuclear radii are given by $R_i = r_0 A_i^{1/3}$, Z_i represents the nuclear charge and μ represents the reduced mass of the system.

In comparing this model with the data, we have chosen the systems formed from the fission of ^{238}U induced by ^4He , ^{12}C , ^{16}O , ^{20}Ne , and ^{40}Ar ions. Experimental values for σ_{CF} were all determined by the fission fragment angular correlation technique^{4,21} under similar assumptions and hence, these studies should form a self-consistent set of results with which to examine the theory.

Experimental values for l_c were determined assuming a triangular distribution of l waves for complete fusion reactions, i.e., the transmission coefficients T_l were taken to be

$$l \leq l_c, \quad T_l = 1,$$

$$l > l_c, \quad T_l = 0.$$

Thus, experimental l_c values could be calculated from the relation

$$\sigma_{\text{CF}} = \pi \lambda^2 (l_c + 1)^2.$$

A more exact approach would be to use a Fermi distribution for the transmission coefficients and equate l_c with the l value at which $T_l = 0.5$. Because of the large angular momenta involved in these reactions, the triangular approximation gives nearly identical results. However, the value of l_c calculated here should realistically be interpreted as representing some region of the l wave distribution over which the probability for complete fusion reactions decreases to zero.

The only adjustable parameter in these calculations involved the choice of r_0 . Wilczyński⁵ used two separate r_0 values in his calculation: $r_0 = 1.20$ fm for the surface tension coefficient and $r_0 = 1.11$ fm for the charge and centrifugal terms. This assumption implies drastic reduction in the cross section for projectiles such as ^{84}Kr and we have instead chosen to use a single self-consistent value for r_0 , appropriate to all three terms. However, it should be pointed out that the resultant r_0 value is smaller than the value of r_0 derived from the semiempirical mass formula, from which the constants a_s and κ were taken. By fitting the data for ^{12}C -, ^{16}O -, ^{20}Ne -, and ^{40}Ar -induced fission of ^{238}U , a value of $r_0 = 1.10$ fm is obtained. Using this

value and an α particle radius of $R_\alpha = 2.08$ fm,²² the values of l_c and σ_{CF} shown in Table II were calculated. The agreement between theory and calculation is generally good, although the ^{12}C and ^{40}Ar points deviate noticeably. However, the ^4He -ion result is surprisingly consistent with the Wilczyński model.

In Fig. 5 the behavior of the complete fusion cross section predicted by the Wilczyński model is compared with the experimental results discussed in Sec. IV A. Although there are rather large uncertainties in the data as they now exist, the results imply that the energy-dependence of the Wilczyński model is not consistent with the data at lower energies. This result is consistent with recent analyses of fusion cross section data by Galin *et al.*²³ and by Gross and Kalinowski,²⁴ which demonstrate that l_c is dependent on bombarding energy. Galin *et al.*²³ parametrize fusion cross sections in terms of a critical radius of approach for the colliding ions, while Gross and Kalinowski²⁴ use a nuclear friction model to calculate l_c . The energy dependence for l_c implied by the results of Fig. 5 are in good qualitative agreement with these latter two calculations.

V. CONCLUSIONS

In summary, the present research demonstrates the importance of reaction mechanism studies to the interpretation of intermediate energy fission data. We find that less than one-half of the total reaction cross section involves complete fusion of target and projectile at a bombarding energy of 140-MeV and that a large fraction of the incomplete fusion events involves linear momentum transfers with 50–90% of the value expected for compound nucleus formation, presumably the result of preequilibrium decay or deep knockout reactions. Based on these results, it is probable that similar effects occur at lower energies to an extent much larger than previously thought. The large fraction of incomplete fusion events compli-

TABLE II. Comparison of experimental values for the critical angular momentum and complete fusion cross section with values calculated using model of Wilczyński (Ref. 5) using $r_0 = 1.10$ fm.

Target	Projectile	σ_{CF} (exp) (mb)	σ_{CF} (calc) (mb)	l_c (exp)	l_c (calc)
^{238}U	140-MeV ^4He	1360	1459	32.5	33.7
^{238}U	125-MeV ^{12}C	1550	1905	56.5	61.8
^{238}U	166-MeV ^{16}O	1490	1476	71.8	71.5
^{238}U	208-MeV ^{20}Ne	1360	1321	84.5	83.4
^{238}U	416-MeV ^{40}Ar	992	669	135	110

cates the analysis of fission data obtained at intermediate energies due to the broad spectrum of fissioning nuclei and excitation energies that result, as well as the difficulty in calculating the orbital angular momentum distribution of the products. Thus, previous conclusions drawn from intermediate energy fission data need to be reevaluated if a knowledge of these quantities is involved. This is particularly true of isomer ratio studies and interpretations of fission fragment angular distribution data. In addition, the decreasing value of $\sigma_{\text{CI}}/\sigma_{\text{R}}$ with increasing energy may explain in part the difficulties encountered in fitting the high energy part of theoretical Γ_n/Γ_f expressions to experimental fission cross section data.²⁵ Our results do show that the fission of nuclides lighter than bismuth occurs largely via compound nucleus formation reactions, which is an important consideration in the study of less fissile systems.

Comparison of our results with the critical angular momentum values calculated using the semiclassical macroscopic models of Wilczyński⁵ and Bass⁶ shows good agreement at high bombarding energies, but the data and theory deviate noticeably at lower energies. However, the experimental re-

sults for l_c using ^4He ions as projectiles are qualitatively the same as the energy-dependent theoretical predictions of Galin²³ and Gross.²⁴ The results imply that such models may be at least approximately valid for intermediate-energy ^4He -ion collisions. However, in order to understand fully the distribution of nuclear species, excitation energies, and angular momenta produced in these reactions, a microscopic calculation which takes into account complete fusion, preequilibrium decay, deep knockout, and transfer reactions is needed.

ACKNOWLEDGMENTS

The authors wish to thank Dr. R. N. Yoder for his assistance with the IBM-360/44 computer system and Dr. W. Johnson and the staff of the Maryland cyclotron for their cooperation in performing these experiments. We also thank Dr. M. M. Minor, Joan Graber, and Pamela Schuster for their assistance with various aspects of this work. Professor H. M. Blann is also acknowledged for several valuable comments concerning intermediate-energy ^4He -ion reactions.

*Work supported in part by U. S. Atomic Energy Commission Contract No. AT(40-1)-4028.

†Present address: Argonne National Laboratory, Argonne, Illinois 60439.

¹J. R. Huizenga and L. G. Moretto, *Annu. Rev. Nucl. Sci.* **22**, 427 (1972).

²T. D. Thomas, *Annu. Rev. Nucl. Sci.* **18**, 343 (1968).

³R. Vandenbosch and J. R. Huizenga, *Nuclear Fission* (Academic, New York, 1973).

⁴T. Sikkeland, E. L. Haines, V. E. Viola, Jr., *Phys. Rev.* **125**, 1350 (1962); T. Sikkeland, V. E. Viola, Jr., in *Proceedings of the Third Conference on Reactions Between Complex Nuclei* (Univ. of California Press, Berkeley, 1963), p. 232.

⁵J. Wilczyński, *Nucl. Phys.* **A216**, 386 (1973).

⁶R. Bass, *Phys. Lett.* **47B**, 139 (1973).

⁷S. Cohen, F. Plasil, and W. J. Swiatecki, in *Proceedings of the Third Conference on Reactions Between Complex Nuclei* (see Ref. 4), p. 325.

⁸B. N. Kalinkin and I. Z. Petkov, *Acta Phys. Pol.* **25**, 265 (1964).

⁹H. M. Blann and F. Plasil, *Phys. Lett.* **29**, 303 (1972); H. M. Blann, in *Proceedings of the Heavy Ion Summer Study, Oak Ridge, 1972* (unpublished), p. 269, CONF-720669.

¹⁰S. S. Kapoor, H. Baba, and S. G. Thompson, *Phys. Rev.* **149**, 965 (1966).

¹¹V. E. Viola, Jr., *et al.*, *Nucl. Phys.* **A174**, 321 (1971).

¹²H. Blann, private communication; M. Blann and F. M.

Lanzafame, *Nucl. Phys.* **A142**, 559 (1970); F. M. Lanzafame and M. Blann, *ibid.* **A142**, 545 (1970).

¹³R. Bimbot and Y. Lebeyec, *J. Phys. (Paris)* **32**, 243 (1971).

¹⁴V. E. Viola, Jr., and T. Sikkeland, *Phys. Rev.* **128**, 767 (1962).

¹⁵J. O. Rasmussen and K. Sugawara-Tanabe, *Nucl. Phys.* **A171**, 497 (1971).

¹⁶F. K. McGowan, *et al.*, *Phys. Rev. Lett.* **27**, 1741 (1971).

¹⁷I. Halpern, private communication; G. Chenevert *et al.*, *Phys. Rev. Lett.* **27**, 434 (1971).

¹⁸V. E. Viola, Jr., M. M. Minor, C. T. Roche, and R. G. Clark, in *Proceedings of the Third International Symposium on Physics and Chemistry of Fission* (IAEA, Vienna, 1973).

¹⁹J. B. Natowitz, E. T. Chulick, and M. N. Namboodiri, *Phys. Rev. C* **6**, 2133 (1972); J. B. Natowitz, *ibid.* **1**, 623 (1970).

²⁰A. M. Zebelman and J. M. Miller, *Phys. Rev. Lett.* **30**, 27 (1973).

²¹T. Sikkeland, *Ark. Fys.* **36**, 539 (1966).

²²R. Hofstadter, *Rev. Mod. Phys.* **28**, 214 (1956).

²³J. Galin, D. Guerreau, M. Lefort, and X. Tarrago, *Phys. Rev. C* **9**, 1018 (1974).

²⁴D. H. E. Gross and H. Kalinowski, *Phys. Lett.* **48B**, 302 (1974).

²⁵A. Khodai-Joopari, University of California Radiation Laboratory Report No. UCRL-16489, 1966 (unpublished).